Generalized Quantum Measurements on a Higher-Dimensional System via Quantum Walks

Xiaowei Wang,[1,*] Xiang Zhan,[2,3,*] Yulin Li,[2] Lei Xiao,[1] Gaoyan Zhu,[1] Dengke Qu,[1] Quan Lin,[1] Yue Yu,[2] and Peng Xue[1,†]

[1]*Beijing Computational Science Research Center, Beijing 100084, China*

[2]*School of Science, Nanjing University of Science and Technology, Nanjing 210094, China*

[3]*MIIT Key Laboratory of Semiconductor Microstructure and Quantum Sensing, Nanjing University of Science and Technology, Nanjing 210094, China*

(Received 31 January 2023; accepted 18 September 2023; published 10 October 2023)

Quantum measurements play a fundamental role in quantum mechanics. Especially, generalized quantum measurements provide a powerful and versatile tool to extract information from quantum systems. However, how to realize them on an arbitrary higher-dimensional quantum system remains a challenging task. Here we propose a simple recipe for the implementation of a general positive-operator valued measurement (POVM) on a higher-dimensional quantum system via a one-dimensional discrete-time quantum walk with a two-dimensional coin. Furthermore, using single photons and linear optics, we realize experimentally a symmetric, informationally complete (SIC) POVM on a three-dimensional system with high fidelity. As an application, we realize a qutrit state tomography with SIC-POVM and confirm that the infidelity scaling achieved by the qutrit SIC-POVM is as good as that based on mutually unbiased bases. Our study paves the way to explore physics and information in higher-dimensional quantum systems and finds applications in various quantum information processing tasks that rely on generalized quantum measurements.

DOI: 10.1103/PhysRevLett.131.150803

Introduction.—Quantum measurement is the interface from quantum systems to classical world [1–3]. As the generalized quantum measurement, positive-operator valued measurement (POVM) offers an efficient method to acquire information that far surpasses the performance of von Neuman projective measurement [1]. A typical and fundamental example is that projective measurement can only discriminate orthogonal states, while POVM is able to discriminate nonorthogonal ones [4–13]. Therefore, POVM is a versatile tool in studying quantum information and fundamental quantum theory [4,11,14–21]. Physically, POVMs correspond to projective measurements on a joint system of the system of interest and an ancilla whose state is known [22,23]. So far, POVMs on a qubit have been realized in a number of different physical systems [6,24–40]. However, POVMs on an arbitrary higher-dimensional quantum system still attract attention.

Among the proposals of qubit POVMs, a feasible and user-friendly recipe is based on a one-dimensional discrete-time quantum walk (QW), which was first proposed by Kurzyński and Wójcik [41] and demonstrated experimentally in photonic systems [39]. Recently, the method has been generalized to implement POVMs on a qudit via QWs with a higher-dimensional coin [42]. However, experimentally realizing QWs with a higher-dimensional coin remains a challenging task.

Here we propose a simple recipe for the implementation of POVMs on an arbitrary higher-dimensional quantum system via the simplest version of QWs, i.e., a one-dimensional QW with just a two-dimensional coin. Our method releases the requirement of a higher-dimensional coin and furthermore is general and efficient, i.e., an arbitrary qudit POVM with m rank-1 elements can be implemented via a $(2m-3)$-step QW. It is general to consider rank-1 elements as an arbitrary higher-rank POVM element can be obtained from rank-1 elements with two procedures of mixing and relabeling [43–48]. Using single photons and linear optics, we realize experimentally a symmetric, informationally complete (SIC) POVM on a qutrit with high fidelity. As an application, we realize a qutrit state tomography and confirm that the infidelity scaling achieved by the qutrit SIC-POVM [49–56] is as good as that based on mutually unbiased bases (MUBs) [57–64].

Relation between POVM and QWs.—Consider $\{E_j\}$ being a POVM with each element E_j, which is a positive semi-definite Hermitian operator, $E_j \succeq 0$. The probability of measuring the jth POVM element on a state ρ is given by $\mathrm{Tr}(E_j\rho)$. A complete set of measurement operators has the resolution of identity, i.e., $\sum_j E_j = \mathbb{1}$ is satisfied. Without loss of generality, we consider the POVM with a complete set of m rank-1 elements as

$$E_j = p_j|\phi_j\rangle\langle\phi_j|, \quad j = 1, \ldots, m. \tag{1}$$

In this case, we have $m \geq d$ and the equality holds if and only if the POVM degenerates to a projective measurement, where d is the dimension of the system.

For one-dimensional QWs [65,66], the Hilbert space of the walker-coin $\mathcal{H}^p \otimes \mathcal{H}^c$ is spanned by the basis $|x, c\rangle = |x\rangle \otimes |c\rangle$ with position $x \in \mathbb{Z}$ and coin $c = \pm 1$. An evolution operator $U_t = SC_t$ for the tth step includes a coin operation

$$C_t = \sum_{x\in\mathbb{Z}} |x\rangle\langle x| \otimes C_t^x, \tag{2}$$

followed by a conditional shift operation

$$S = \sum_{x\in\mathbb{Z}, c=\pm 1} |x + c\rangle\langle x| \otimes |c\rangle\langle c|. \tag{3}$$

A projective measurement $P = |x, c\rangle\langle x, c|$ on the evolved state $|\psi_t\rangle = \prod_{i=1}^t U_i|\psi_0\rangle$ of a t-step QW is equivalent to the measurement $P' = |\psi_t^{x,c}\rangle\langle\psi_t^{x,c}|$ on the initial state $|\psi_0\rangle$, where $|\psi_t^{x,c}\rangle = \prod_{i=1}^t U_i^\dagger |x, c\rangle$. When the initial state is confined to finite positions $x' = 0, \ldots, d-1$, the probability of the projective measurement P on $|\psi_t\rangle$ is also equivalent to that of measuring the POVM element $E = p_t^{x,c}|\bar{\phi}_t^{x,c}\rangle\langle\bar{\phi}_t^{x,c}|$ on $|\psi_0\rangle$ [22,23], where $p_t^{x,c} = \||\phi_t^{x,c}\rangle\|^2$, $|\bar{\phi}_t^{x,c}\rangle = |\phi_t^{x,c}\rangle/\sqrt{p_t^{x,c}}$, and $|\phi_t^{x,c}\rangle = \sum_{x'=0}^{d-1}\sum_{c='\pm 1}\langle x', c'|\psi_t^{x,c}\rangle|x', c'\rangle$ is an orthogonal projection of $|\psi_t^{x,c}\rangle$ to a subspace. That is, the probability satisfies

$$P(x, c, t) = \langle\psi_t|P|\psi_t\rangle = \langle\psi_0|P'|\psi_0\rangle = \langle\psi_0|E|\psi_0\rangle. \tag{4}$$

Generation of arbitrary rank-1 POVM elements on qudit.—To realize a d-dimensional POVM with a complete set of m rank-1 elements as Eq. (1), our idea is iteratively implementing unitary operations followed by projective measurements. The main task of our method is to determine the parameters in the operations and measurements. In principle, the dimension of each unitary operation is d. After the first $j-1$ iterations, elements $E_1, \ldots, E_{j-1}$ are implemented, the support of the system after the $(j-1)$th iteration is $\mathrm{supp}(\mathbb{1} - \sum_{j'=1}^{j-1} E_{j'}) = \mathrm{supp}(\sum_{j'=j}^m E_{j'})$. The effective dimension of the system after the $(j-1)$th iteration is equal to the rank of the sum of elements from E_j to E_m

$$r_j \equiv \mathrm{rank}\left(\sum_{j'=j}^m E_{j'}\right), \tag{5}$$

and $r_1 = \mathrm{rank}(\mathbb{1}) = d$ and $r_m = \mathrm{rank}(E_m) = 1$.

Moreover, two neighboring ranks satisfy either $r_j = r_{j+1}$ or $r_j = r_{j+1} + 1$. When $r_j = r_{j+1} + 1$, there must be a state ρ satisfying $\rho \in \mathrm{supp}(\sum_{j'=j}^m E_{j'})$ and $\rho \notin \mathrm{supp}(\sum_{j'=j+1}^m E_{j'})$. For ρ, we have $\mathrm{Tr}(E_j\rho) \neq 0$ and $\mathrm{Tr}(\sum_{j'=j+1}^m E_{j'}\rho) = 0$, which can be used as a signature of the decreasing of the rank. Now we are ready to introduce our algorithm for realizing POVMs.

First, we recall that the rank-1 elements are of the form in Eq. (1) and encode a d-dimensional system into $n = \lceil d/2 \rceil$ positions of the walker and $|c\rangle = |\pm 1\rangle$ into coin states. If d is even, we use the qudit basis $|x, c\rangle$ with $x = 1, 3, \ldots, 2n-1$. If d is odd, we use $|2n-1, +1\rangle$ and $|x, c\rangle$ with $x = 1, 3, \ldots, 2n-3$. The QW network is built by starting with a blank grid, and putting the coin operation C_t^x at position x in step t. In the following, we show the algorithm to obtain specific C_t^x, x, and t: (S1) Initiate the QW at position $x = 1, 3, \ldots, 2n-1$ with the coin state, corresponding to the qudit state to be measured. (S2) Apply coin operation $\sigma_x = \left(\begin{smallmatrix}0&1\\1&0\end{smallmatrix}\right)$ at position $x = 0$ in all steps t and at position $x = d$ in step $t \leq d-1$. (S3) For $j = 1, \ldots, m-1$ (m is the number of the elements): (a) For $k = 1, \ldots, r_j$, apply the coin operation $R_{j,k}$ at position $x = k$ in step $t = k + 2j - 2$. (b) Measure the walker at position $x = r_{j+1} + 1$ after step $t = r_{j+1} + 2j - 2$, which is equivalent to the measurement of the POVM element E_j. (S4) Apply the coin operations as $\mathbb{1} = \left(\begin{smallmatrix}1&0\\0&1\end{smallmatrix}\right)$ elsewhere. (S5) Measure the walker at position $x = 0$ after step $t = 2m-3$, which is equivalent to the measurement of the POVM element E_m.

The position and steps for operations $R_{j,k}$ are illustrated in Fig. 1(a). In the Supplemental Material [67], we prove

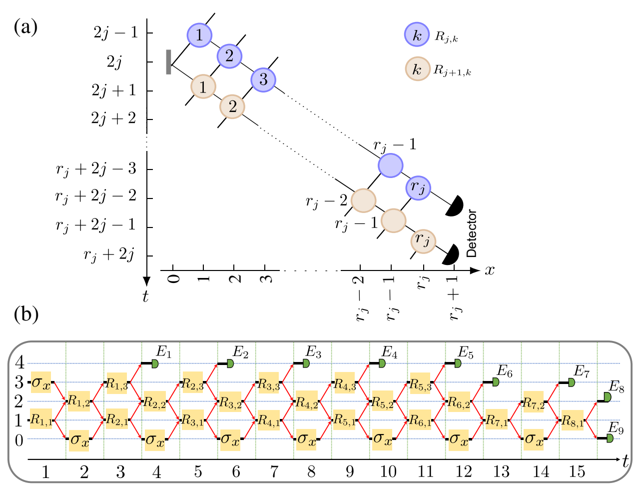

FIG. 1. (a) Illustration of the algorithm for the generation of an arbitrary rank-1 POVM on a qudit. Coin operations $R_{j,k}$ for $k = 1, \ldots, r_j$. (b) Realization of a qutrit SIC-POVM via a 15-step QW. The coin qubit and the walker in positions are taken as a qutrit of interest, whereas the other positions of the walker act as ancillae. Position-dependent coin operations are specified based on the algorithm. Some coins at certain positions are not shown as those positions are not reachable by a QW from the used initial state. The 9 detectors E_i correspond to the 9 outcomes of the qutrit SIC-POVM.

that the operators can always be chosen in such a way as to implement any desired POVM.

A SIC-POVM on a qutrit.—To demonstrate our algorithm, we consider a SIC-POVM [49–56] on a qutrit as an example. There are $m = d^2$ elements of a SIC-POVM on a d-dimensional system, $E_j = |\phi_j\rangle\langle\phi_j|/d$ with equal pairwise overlaps $|\langle\phi_{j'}|\phi_{j''}\rangle|^2 = (d\delta_{j'j''} + 1)/(d+1)$. For a qutrit system ($d = 3$), all SIC-POVMs are covariant with the Heisenberg-Weyl group, which can be generated by the shift operator $X = |0\rangle\langle 2| + |1\rangle\langle 0| + |2\rangle\langle 1|$ and the phase operator $Z = \sum_{k=0}^{2} e^{ik(2\pi/3)}|k\rangle\langle k|$. Without loss of generality, we choose

$$|\phi_j\rangle = X^p Z^q |\phi_f\rangle, \quad p,q = 0,1,2, \quad j = 3p + q + 1, \tag{6}$$

where $|\phi_f\rangle = (|1\rangle - |2\rangle)/\sqrt{2}$ denotes the fiducial state. According to Eq. (5), we have $r_1 = r_2 = \cdots = r_6 = 3$, $r_7 = r_8 = 2$, $r_9 = 1$.

To realize such a qutrit SIC-POVM via QWs, we encode the system into $n = 2$ positions of the walker. That is, the qutrit basis $\{|0\rangle, |1\rangle, |2\rangle\}$ is encoded into the walker-coin states $\{|1,-1\rangle, |1,+1\rangle, |3,+1\rangle\}$. Based on the algorithm, the coin operation σ_x is taken at position $x = 0$ in all steps and at position $x = 3$ in steps $t = 1, 2$. Let us consider the POVM element $E_{j=1}$ first. We have $r_1 = r_2 = 3$ for $j = 1$. Then the coin operations are $R_{j=1,k=1}$ at position $x = 1$ in step $t = 1$, $R_{j=1,k=2}$ at position $x = 2$ in step $t = 2$, and $R_{j=1,k=3}$ at position $x = 3$ in step $t = 3$, respectively. The walker at position $x = 4$ is measured after $t = 3$ and the probability is equivalent to that of POVM element E_1 on the initial state. The particular forms of the coin operations $R_{1,1}$, $R_{1,2}$, and $R_{1,3}$ are specified in the Supplemental Material [67]. The other elements can be realized similarly based on the algorithm.

As illustrated in Fig. 1(b), the coin operations at the positions $x = 1$ and $x = 3$ in the first step are $R_{1,1}$ and σ_x, respectively. According to our algorithm, for the SIC-POVM on a qutrit in Eq. (6), we have $R_{1,1} = \mathbb{1}$ [67]. Therefore, the first step works as a permutation of the basis that can be combined with the initial state preparation. Then the basis states of the qutrit are encoded into the walker-coin states $\{|0,-1\rangle, |2,+1\rangle$, and $|2,-1\rangle$ instead. With these choices, the SIC-POVM can be realized via a 14-step QW.

Experimental realization.—The experimental setup is illustrated in Fig. 2. The coin and position states of the walker are encoded into the polarizations and spatial modes of the heralded single photon, respectively.

The position-dependent coin operations C_t^x (including σ_x and $R_{j,k}$) are specified by the algorithm and can be realized by wave plates placed in the specific spatial modes. The conditional position shift operation is realized by a cascaded interferometric network involving the birefringent calcite beam displacers (BDs), whose optical axes are cut so that the vertically polarized photons are transmitted

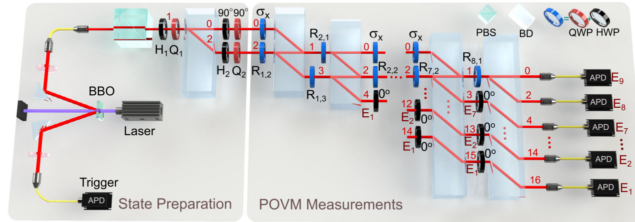

FIG. 2. Schematic of the experimental setup. Heralded single photons are generated via type-I spontaneous parametric down-conversion and prepared in 9 different qutrit states vis a beam displacer (BD) and wave plates (H_1, Q_1, H_2, and Q_2). Combined with the first coin operation, the basis states are encoded by the coin and the walker in positions 0 and 2. Then the single photons undergo a POVM device based on a QW with a two-dimensional coin, which includes coin operations realized by wave plates and conditional shift operations realized by BDs. Finally, photons are detected by avalanche photodiodes (APDs) via a coincidence with the trigger photons. Each of the 9 APDs corresponds to an outcome of a POVM element.

directly and the horizontally polarized photons are shifted to the adjacent spatial mode, respectively. The photons are detected by avalanche photodiodes (APDs) via a coincidence with the trigger photons in a 3 ns time window. Total coincidence counts are about 12000 over a collection time of 8 s. There are 9 output ports, each of which corresponds to an outcome of a POVM element.

To verify the experimental implementation of the qutrit SIC-POVM, we reconstruct the matrix forms of the POVM elements via quantum measurement tomography. First, we prepare the 9 basis states as input states

$$|\varphi_1\rangle = \begin{pmatrix} 0 \\ 1 \\ 0 \end{pmatrix}, \quad |\varphi_2\rangle = \begin{pmatrix} 0 \\ 0 \\ 1 \end{pmatrix}, \quad |\varphi_3\rangle = \frac{1}{\sqrt{2}}\begin{pmatrix} 0 \\ 1 \\ i \end{pmatrix},$$
$$|\varphi_4\rangle = \frac{1}{\sqrt{2}}\begin{pmatrix} 0 \\ 1 \\ 1 \end{pmatrix}, \quad |\varphi_5\rangle = \begin{pmatrix} 1 \\ 0 \\ 0 \end{pmatrix}, \quad |\varphi_6\rangle = \frac{1}{\sqrt{2}}\begin{pmatrix} i \\ -1 \\ 0 \end{pmatrix},$$
$$|\varphi_7\rangle = \frac{1}{\sqrt{2}}\begin{pmatrix} i \\ 0 \\ i \end{pmatrix}, \quad |\varphi_8\rangle = \frac{1}{\sqrt{2}}\begin{pmatrix} 1 \\ 0 \\ i \end{pmatrix}, \quad |\varphi_9\rangle = \frac{1}{\sqrt{2}}\begin{pmatrix} 1 \\ -1 \\ 0 \end{pmatrix}. \tag{7}$$

For each input state, we obtain the probability distribution $P(|\varphi_i\rangle) = N_k / \sum_{k=1,\ldots,9} N_k$ after the input state goes through the setup of POVM, where N_k is the number of the photons being detected at APD E_k as illustrated in Fig. 2. The probability distributions of the 9 basis states are shown in Fig. 3. With the probability distributions, we can reconstruct the matrix form of each POVM element via the maximum likelihood method [67,74]. The results are shown in Fig. 4. We report a

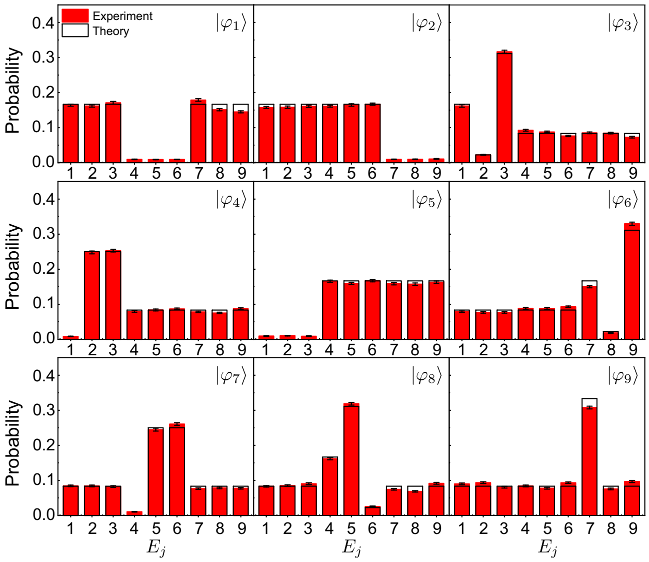

FIG. 3. Probabilities of the photons being detected at each APD after the POVM performed on the basis state $|\varphi_i\rangle$ with $i = 1, \ldots, 9$. Solid and hollow bars represent the experimental results and their theoretical predictions, respectively. Error bars indicate the statistical uncertainty, obtained via error propagation assuming Poissonian statistics.

figure of merit to characterize aspects of our experimental realization of the qutrit SIC-POVM—fidelity $F = (1/d^2)\left(\sum_{j=1}^{m}\sqrt{F_j}\sqrt{\mathrm{Tr}(E_j^{\mathrm{exp}})\mathrm{Tr}(E_j^{\mathrm{th}})}\right)^2$, where $F_j = \left(\mathrm{Tr}\left[\sqrt{\sqrt{[E_j^{\mathrm{exp}}/\mathrm{Tr}(E_j^{\mathrm{exp}})]}[E_j^{\mathrm{th}}/\mathrm{Tr}(E_j^{\mathrm{th}})]\sqrt{[E_j^{\mathrm{exp}}/\mathrm{Tr}(E_j^{\mathrm{exp}})]}}\right]\right)^2$. For overall 9 input states, we observe $F = 0.949 \pm 0.002$.

Here we compare our method with some previous approaches [75–79] for implementing POVMs. Realizing a POVM with d^2 outcomes on a d-dimensional quantum system, the standard realization via the Neumark extension [75–77] requires a $d^2 \times d^2$ unitary transform and $d^2(d^2-1)/2$ operations between pairs of basis states. The realization using just a single extra degree of freedom proposed by Wang and Ying in [78] requires a $(d+1)\times(d+1)$ unitary transform and $d^2(d^2-1)/2$ operations between pairs of basis states. A binary search tree for POVM proposed by Andersson and Oi [79] requires a $2d \times 2d$ transform and $\lceil \log_2 d^2 \rceil d(2d-1)$ operations. By using our method, a $d \times d$ transform and $\lceil d/2 \rceil (2d^2-3)$ operations are needed [67]. Thus, our method shows potential advantages compared to the previous ones [75–79].

An application of SIC-POVMs.—As an application, we realize qutrit state tomography with SIC-POVM. We choose different qutrit states ρ. After the SIC-POVM is performed, the probabilities are estimated from the frequencies of the repeated measurements. Then the states can be reconstructed via the maximum likelihood method [67]. The quantum infidelity $1 - F' = 1 - \mathrm{Tr}(\sqrt{\sqrt{\rho}\rho'\sqrt{\rho}})^2$ between a state ρ and its estimate ρ' can be used to quantify the accuracy of a measurement. Figure 5 shows the quantum infidelity about the dependence on the number of copies of the state of interest N, which is equivalent to the number of photons. We choose three different qutrit states as examples and fit both experimental and simulated data to power laws of the form βN^{-q}, and find $q_{\mathrm{exp}} = 0.886 \pm 0.012$ (for experiment data) and $q_{\mathrm{sim}} = 1.009 \pm 0.011$ (for simulated data) for $|\varphi_1\rangle$, $q_{\mathrm{exp}} = 0.402 \pm 0.052$ and $q_{\mathrm{sim}} = 0.538 \pm 0.020$ for $|\varphi_4\rangle$, and $q_{\mathrm{exp}} = 0.407 \pm 0.019$ and $q_{\mathrm{sim}} = 0.508 \pm 0.021$ for $|\varphi_8\rangle$, respectively. The infidelity scaling achieved by the qutrit SIC-POVM is state dependent.

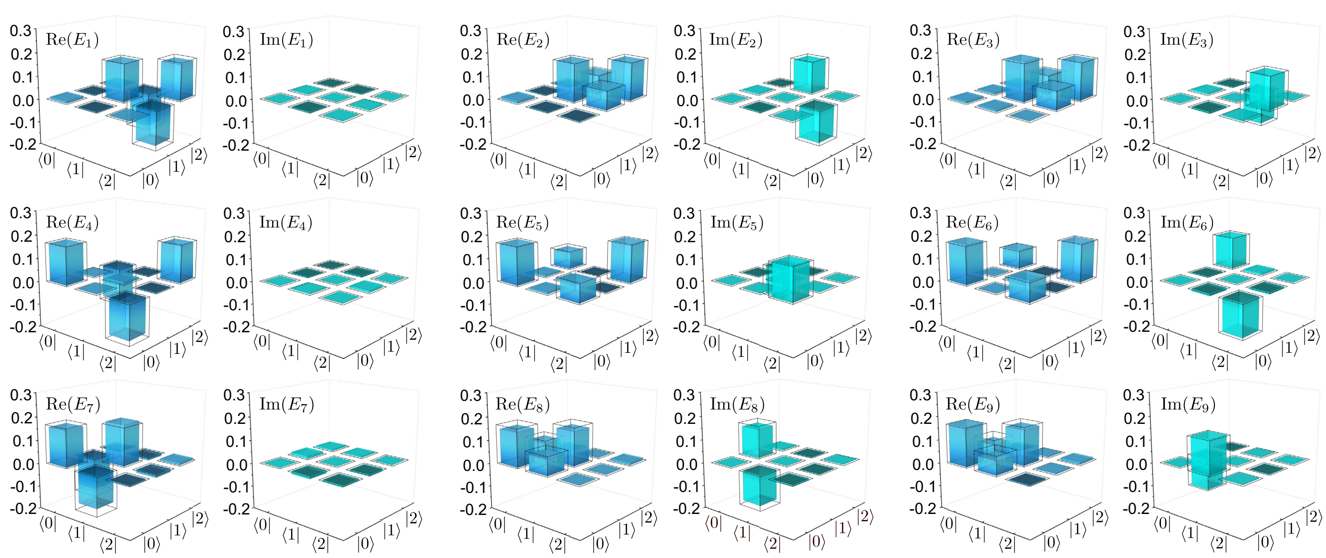

FIG. 4. Matrix forms of the elements E_j of a qutrit SIC-POVM. Real and imaginary parts of the matrix forms of the 9 reconstructed POVM elements are plotted by solid bars, while hollow bars represent their theoretical predictions.

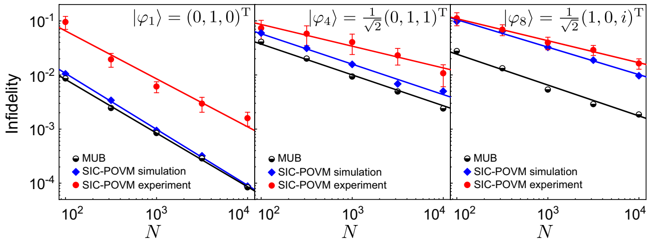

FIG. 5. Infidelity versus N for two different measure methods: a qutrit SIC-POVM and MUBs. We choose three different states: $|\varphi_1\rangle$, $|\varphi_4\rangle$, and $|\varphi_8\rangle$, for examples. Both experimental and numerical results for SIC-POVM and numerical results for MUBs are shown for comparison. Experimental and numerical results are both shown. Numerical results are obtained by Monte Carlo simulations. Each data point is the average of 1000 repetitions.

For comparison, we also show the numerical results achieved by the measurement of the full set of MUBs [57–64] for qutrit states. We fit the simulated MUB data to power laws of the form βN^{-q}, and obtain $q = 0.998 \pm 0.008$, 0.570 ± 0.017, 0.570 ± 0.022 for the states $|\varphi_1\rangle$, $|\varphi_4\rangle$ and $|\varphi_8\rangle$, respectively. As illustrated in Fig. 5, the infidelity scaling achieved by the qutrit SIC-POVM is as good as that by MUBs.

Conclusion.—We present a simple proposal for implementing an arbitrary higher-dimensional POVM by the simplest version of QWs, i.e., a QW with just a two-dimensional coin. Our proposal releases the requirement of a higher-dimensional coin and furthermore is general and efficient. All coin operations can be determined algorithmically. Using single photons and linear optics, we realize experimentally a SIC-POVM on a qutrit with high fidelity. The results prove that the infidelity scaling achieved by the qutrit SIC-POVM is as good as that by MUBs. Our study paves the way to explore physics and information in higher-dimensional quantum systems and will be applied in various quantum information processing tasks that rely on generalized quantum measurements.

This work is supported by the National Natural Science Foundation of China (Grants No. 92265209, No. 12025401, No. 12004184, No. 12088101).

*These authors contributed equally to this work.
†gnep.eux@gmail.com

[1] M. A. Nielson and I. L. Chuang, *Quantum Computation and Quantum Information*, 2nd ed. (Cambridge University Press, Cambridge, England, 2010).
[2] A. I. Lvovsky and M. G. Raymer, Continuous-variable optical quantum-state tomography, Rev. Mod. Phys. **81**, 299 (2009).
[3] V. Giovannetti, S. Lloyd, and L. Maccone, Advances in quantum metrology, Nat. Photonics **5**, 222 (2011).
[4] S. Massar and S. Popescu, Optimal extraction of information from finite quantum ensembles, Phys. Rev. Lett. **74**, 1259 (1995).
[5] A. Peres and D. R. Terno, Optimal distinction between non-orthogonal quantum states, J. Phys. A **31**, 7105 (1998).
[6] R. B. M. Clarke, A. Chefles, S. M. Barnett, and E. Riis, Experimental demonstration of optimal unambiguous state discrimination, Phys. Rev. A **63**, 040305(R) (2001).
[7] M. Dušek and V. Bužek, Quantum-controlled measurement device for quantum-state discrimination, Phys. Rev. A **66**, 022112 (2002).
[8] S. M. Barnett and S. Croke, Quantum state discrimination, Adv. Opt. Photonics **1**, 238 (2009).
[9] G. A. Steudle, S. Knauer, U. Herzog, E. Stock, V. A. Haisler, D. Bimberg, and O. Benson, Experimental optimal maximum-confidence discrimination and optimal unambiguous discrimination of two mixed single-photon states, Phys. Rev. A **83**, 050304(R) (2011).
[10] J. Bae and L.-C. Kwek, Quantum state discrimination and its applications, J. Phys. A **48**, 083001 (2015).
[11] H. Zhu and M. Hayashi, Universally Fisher-symmetric informationally complete measurements, Phys. Rev. Lett. **120**, 030404 (2018).
[12] J. Shang, A. Ali, H. Zhu, and G. Otfried, Enhanced entanglement criterion via symmetric informationally complete measurements, Phys. Rev. A **98**, 022309 (2018).
[13] F. Bischof, H. Kampermann, and D. Bruß, Resource theory of coherence based on positive-operator-valued measures, Phys. Rev. Lett. **123**, 110402 (2019).
[14] A. K. Ekert, B. Huttner, G. M. Palma, and A. Peres, Eavesdropping on quantum-cryptographical systems, Phys. Rev. A **50**, 1047 (1994).
[15] H. E. Brandt, J. M. Myers, and S. J. Lomonaco, Aspects of entangled translucent eavesdropping in quantum cryptography, Phys. Rev. A **56**, 4456 (1997).
[16] A. Bisio, G. Chiribella, G. M. D'Ariano, S. Facchini, and P. Perinotti, Optimal quantum tomography of states, measurements, and transformations, Phys. Rev. Lett. **102**, 010404 (2009).
[17] D. Petz and L. Ruppert, Optimal quantum-state tomography with known parameters, J. Phys. A **45**, 085306 (2012).
[18] C. C. W. Lim, C. Portmann, M. Tomamichel, R. Renner, and N. Gisin, Device-independent quantum key distribution with local Bell test, Phys. Rev. X **3**, 031006 (2013).
[19] C. A. Fuchs and R. Schack, Quantum-Bayesian coherence, Rev. Mod. Phys. **85**, 1693 (2013).
[20] X. Zhan, G. C. Eric, J. Li, Z. Bian, Y. Zhang, H. M. Wiseman, and P. Xue, Experimental generalized contextuality with single-photon qubits, Optica **4**, 966 (2017).
[21] Z. Hou, J.-F. Tang, J. Shang, H. Zhu, J. Li, Y. Yuan, K.-D. Wu, G.-Y. Xiang, C.-F. Li, and G.-C. Guo, Deterministic realization of collective measurements via photonic quantum walks, Nat. Commun. **9**, 1414 (2018).
[22] M. A. Naimark, A. I. Loginov, and V. S. Shul'man, Non-self-adjoint operator algebras in Hilbert space, J. Sov. Math. **5**, 250 (1976).
[23] A. Peres, Neumark's theorem and quantum inseparability, Found. Phys. **20**, 1441 (1990).
[24] P.-X. Chen, J. A. Bergou, S.-Y. Zhu, and G.-C. Guo, Ancilla dimensions needed to carry out positive-operator-valued measurement, Phys. Rev. A **76**, 060303(R) (2007).

[25] G. Brida, L. Ciavarella, I. P. Degiovanni, M. Genovese, A. Migdall, M. G. Mingolla, M. G. A. Paris, F. Piacentini, and S. V. Polyakov, Ancilla-assisted calibration of a measuring apparatus, Phys. Rev. Lett. **108**, 253601 (2012).

[26] P. J. Mosley, S. Croke, I. A. Walmsley, and S. M. Barnett, Experimental realization of maximum confidence quantum state discrimination for the extraction of quantum information, Phys. Rev. Lett. **97**, 193601 (2006).

[27] A. Ling, K. P. Soh, A. Lamas-Linares, and C. Kurtsiefer, Experimental polarization state tomography using optimal polarimeters, Phys. Rev. A **74**, 022309 (2006).

[28] Z. E. D. Medendorp, F. A. Torres-Ruiz, L. K. Shalm, G. N. M. Tabia, C. A. Fuchs, and A. M. Steinberg, Experimental characterization of qutrits using symmetric informationally complete positive operato-valued measurements, Phys. Rev. A **83**, 051801(R) (2011).

[29] G. N. M. Tabia, Experimental scheme for qubit and qutrit symmetric informationally complete positive operator-valued measurements using multiport devices, Phys. Rev. A **86**, 062107 (2012).

[30] G. Waldherr, A. C. Dada, P. Neumann, F. Jelezko, E. Andersson, and J. Wrachtrup, Distinguishing between nonorthogonal quantum states of a single nuclear spin, Phys. Rev. Lett. **109**, 180501 (2012).

[31] Y. Liu and J. X. Cui, Realization of Kraus operators and POVM measurements using a duality quantum computer, Chin. Sci. Bull. **59**, 2298 (2014).

[32] Y. S. Yordanov and C. H. W. Barnes, Implementation of a general single-qubit positive operator-valued measure on a circuit-based quantum computer, Phys. Rev. A **100**, 062317 (2019).

[33] M. Oszmaniec, L. Guerini, P. Wittek, and A. Acín, Simulating positive-operator-valued measures with projective measurements, Phys. Rev. Lett. **119**, 190501 (2017).

[34] M. Oszmaniec, F. B. Maciejewski, and Z. Puchała, Simulating all quantum measurements using only projective measurements and postselection, Phys. Rev. A **100**, 012351 (2019).

[35] H. Sosa-Martinez, N. K. Lysne, C. H. Baldwin, A. Kalev, I. H. Deutsch, and P. S. Jessen, Experimental study of optimal measurements for quantum state tomography, Phys. Rev. Lett. **119**, 150401 (2017).

[36] A. Zhang, J. Xie, H. Xu, K. Zheng, H. Zhang, Y.-T. Poon, V. Vedral, and L. Zhang, Experimental self-characterization of quantum measurements, Phys. Rev. Lett. **124**, 040402 (2020).

[37] N. Lupu-Gladstein, Y. B. Yilmaz, D. R. M. Arvidsson-Shukur, A. Brodutch, A. O. T. Pang, A. M. Steinberg, and N. Y. Halpern, Negative quasiprobabilities enhance phase estimation in quantum-optics experiment, Phys. Rev. Lett. **128**, 220504 (2022).

[38] N. Bent, H. Qassim, A. A. Tahir, D. Sych, G. Leuchs, L. L. Sánchez-Soto, E. Karimi, and R. W. Boyd, Experimental realization of quantum tomography of photonic qudits via symmetric informationally complete positive operator-valued measures, Phys. Rev. X **5**, 041006 (2015).

[39] Z. Bian, J. Li, H. Qin, X. Zhan, R. Zhang, B. C. Sanders, and P. Xue, Realization of single-qubit positive-operator-valued measurement via a one-dimensional photonic quantum walk, Phys. Rev. Lett. **114**, 203602 (2015).

[40] Y. Zhao, N. Yu, P. Kurzyński, G. Xiang, C.-F. Li, and G.-C. Guo, Experimental realization of generalized qubit measurements based on quantum walks, Phys. Rev. A **91**, 042101 (2015).

[41] P. Kurzyński and A. Wójcik, Quantum walk as a generalized measuring device, Phys. Rev. Lett. **110**, 200404 (2013).

[42] Z. Li, H. Zhang, and H. Zhu, Implementation of generalized measurements on a qudit via quantum walks, Phys. Rev. A **99**, 062342 (2019).

[43] H. Martens and W. M. de Muynck, Nonideal quantum measurements, Found. Phys. **20**, 255 (1990).

[44] G. M. D'Ariano, P. L. Presti, and P. Perinotti, Classical randomness in quantum measurements, J. Phys. A **38**, 5979 (2005).

[45] F. Buschemi, M. Keyl, G. M. D'Ariano, P. Perinotti, and R. F. Werner, Clean positive operator valued measures, J. Math. Phys. (N.Y.) **46**, 082109 (2005).

[46] E. Haapasalo, T. Heinosaari, and J. P. Pellonpää, Quantum measurements on finite dimensional systems: relabeling and mixing, Quantum Inf. Process. **11**, 1751 (2012).

[47] G. Sentís, B. Gendra, S. D. Bartlett, and A. C. Doherty, Decomposition of any quantum measurement into extremals, J. Phys. A **46**, 375302 (2013).

[48] T. Singal, F. B. Maciejewski, and M. Oszmaniec, Implementation of quantum measurements using classical resources and only a single ancillary qubit, npj Quantum Inf. **8**, 82 (2022).

[49] J. M. Renes, R. Blume-Kohout, A. J. Scott, and C. M. Caves, Symmetric informationally complete quantum measurements, J. Math. Phys. (N.Y.) **45**, 2171 (2004).

[50] G. Zauner, Quantum designs: Foundations of a noncommutative design theory, Int. J. Quantum. Inform. **09**, 445 (2011).

[51] C. A. Fuchs, M. C. Hoang, and B. C. Stacey, The SIC question: History and state of play, Axioms **6**, 21 (2017).

[52] A. J. Scott and M. Grassl, Symmetric informationally complete positive-operator-valued measures: A new computer study, J. Math. Phys. (N.Y.) **51**, 042203 (2010).

[53] H. Zhu, Quasiprobability representations of quantum mechanics with minimal negativity, Phys. Rev. Lett. **117**, 120404 (2016).

[54] I. J. Geng, K. Golubeva, and G. Gour, What are the minimal conditions required to define a symmetric informationally complete generalized measurement?, Phys. Rev. Lett. **126**, 100401 (2021).

[55] W. M. Pimenta, B. Marques, T. O. Maciel, R. O. Vianna, A. Delgado, C. Saavedra, and S. Padua, Minimum tomography of two entangled qutrits using local measurements of one-qutrit symmetric informationally complete positive operator-valued measure, Phys. Rev. A **88**, 012112 (2013).

[56] A. Tavakoli, I. Bengtsson, N. Gisin, and J. M. Renes, Compounds of symmetric informationally complete measurements and their application in quantum key distribution, Phys. Rev. Res. **2**, 043122 (2020).

[57] W. K. Wootters and B. D. Fields, Optimal state-determination by mutually unbiased measurements, Ann. Phys. (N.Y.) **191**, 363 (1989).

[58] T. Durt, B. G. Englert, I. Bengtsson, and K. Życzkowski, On mutually unbiased bases, Int. J. Quantum. Inform. **08**, 535 (2010).

[59] R. B. A. Adamson and A. M. Steinberg, Improving quantum state estimation with mutually unbiased bases, Phys. Rev. Lett. **105**, 030406 (2010).

[60] D. Giovannini, J. Romero, J. Leach, A. Dudley, A. Forbes, and M. J. Padgett, Characterization of high-dimensional entangled systems via mutually unbiased measurements, Phys. Rev. Lett. **110**, 143601 (2013).

[61] A. Fernández-Pérez, A. B. Klimov, and C. Saavedra, Quantum process reconstruction based on mutually unbiased basis, Phys. Rev. A **83**, 052332 (2011).

[62] D. Sauerwein, C. Macchiavello, L. Maccone, and B. Kraus, Multipartite correlations in mutually unbiased bases, Phys. Rev. A **95**, 042315 (2017).

[63] P. Erker, M. Krenn, and M. Huber, Quantifying high dimensional entanglement with two mutually unbiased bases, Quantum **1**, 22 (2017).

[64] A. Tavakoli, M. Farkas, D. Rosset, J.-D. Bancal, and J. Kaniewski, Mutually unbiased bases and symmetric informationally complete measurements in Bell experiments, Sci. Adv. **7**, eabc3847 (2021).

[65] Y. Aharonov, L. Davidovich, and N. Zagury, Quantum random walks, Phys. Rev. A **48**, 1687 (1993).

[66] J. Kempe, Quantum random walks: An introductory overview, Contemp. Phys. **44**, 307 (2003).

[67] See Supplemental Material at http://link.aps.org/supplemental/10.1103/PhysRevLett.131.150803 for details on the determination of the coin parameters, the proof of universality, quantum state tomography and quantum measurement tomography, comparison with some previous approaches as well as additional experimental details, which includes Refs. [68–73].

[68] M. Paris and J. Rehacek, *Quantum State Estimation* (Springer Berlin, Heidelberg, 2004).

[69] K. Banaszek, G. M. D'Ariano, M. G. A. Paris, and M. F. Sacchi, Maximum-likelihood estimation of the density matrix, Phys. Rev. A **61**, 010304(R) (1999).

[70] D. F. V. James, P. G. Kwiat, W. J. Munro, and A. G. White, Measurement of qubits, Phys. Rev. A **64**, 052312 (2001).

[71] R. Jozsa, Fidelity for mixed quantum states, J. Mod. Opt. **41**, 2315 (1994).

[72] L. Zhang, A. Datta, H. B. Coldenstrodt-Ronge, X.-M. Jin, J. Eisert, M. B. Plenio, and I. A. Walmsley, Recursive quantum detector tomography, New J. Phys. **14**, 115005 (2012).

[73] D. N. Biggerstaff, R. Kaltenbaek, D. R. Hamel, G. Weihs, T. Rudolph, and K. J. Resch, Cluster-state quantum computing enhanced by high-fidelity generalized measurements, Phys. Rev. Lett. **103**, 240504 (2009).

[74] J. Fiurášek, Maximum-likelihood estimation of quantum measurement, Phys. Rev. A **64**, 024102 (2001).

[75] A. Peres, *Quantum Theory: Concepts and Methods* (Kluwer Academic, Dordrecht, 1995).

[76] M. Reck, A. Zeilinger, H. J. Bernstein, and P. Bertani, Experimental realization of any discrete unitary operator, Phys. Rev. Lett. **73**, 58 (1994).

[77] W. R. Clements, P. C. Humphreys, B. J. Metcalf, W. S. Kolthammer, and I. A. Walsmley, Optimal design for universal multiport interferometers, Optica **3**, 1460 (2016).

[78] G. Wang and M. Ying, Realization of positive-operator-valued measures by projective measurements without introducing ancillary dimensions, arXiv:quant-ph/0608235.

[79] E. Andersson and D. K. L. Oi, Binary search trees for generalized measurements, Phys. Rev. A **77**, 052104 (2008).